Communications in Physics, Vol. 29, No. 2 (2019), pp. 189-196
DOI:10.15625/0868-3166/29/2/13762

INVESTIGATION OF SOME CHARACTERIZATIONS OF BLACK TiO_2 NANOTUBES VIA SPECTROSCOPIC METHODS

NGUYEN TRUONG THO[1,2], CAO MINH THI[2], LE VAN HIEU[1] AND PHAM VAN VIET[1,†]

[1]*Faculty of Materials Science and Technology, University of Science – VNU-HCM, 227 Nguyen Van Cu street, District 5, Ho Chi Minh city, Vietnam*

[2]*Ho Chi Minh City University of Technology (HUTECH), 475A Dien Bien Phu street, Binh Thanh District, Ho Chi Minh city, Vietnam*

[†]*E-mail:* pvviet@hcmus.edu.vn

Received 17 April 2019
Accepted for publication 20 June 2019
Published 27 June 2019

Abstract. *Black TiO_2 with substantial Ti^{3+} and oxygen vacancies exhibit an excellent photoelectrochemical water-splitting performance due to the improvement of charge transport by boosting visible light harvesting. In this study, black TiO_2 nanotube arrays synthesized by the anodization method, and then, they have been investigated some characterizations by spectroscopic methods such as UV-visible reflectance (UV-vis DRS), Fourier-transform infrared spectroscopy (FTIR), Raman spectroscopy, and photoluminescence spectrum. The results showed that some highlighted properties of the black TiO_2 nanotube arrays could be applied for efficient water splitting by sunlight.*

Keywords: black TiO_2, spectroscopic technique, water-splitting, photocatalysis.

Classification numbers: 29.30.-h.

I. INTRODUCTION

Photoelectrochemical (PEC) and electrochemical water-splitting by a TiO_2 electrode is regarded as one of the most promising approaches for clean fuel production such as hydrogen and oxygen [1, 2]. Notably, one dimensional oriented TiO_2 nanotubes (TNAs) which were prepared

by the electrochemical anodization have been demonstrated to be efficient photoanodes for the PEC cells [3]. However, the pristine TNAs have a large band gap energy (about 3.3-3.78 eV for anatase phase at room temperature) leading to weak light harvesting to utilize visible or infrared light, and the electron-hole recombination rate is too rapid causing the insufficient PEC performance [4]. Previous publications relating using TNAs for the PEC are usually low efficiency (about 1%) [5,6]. The structure modification of TiO_2 have been investigating by many approaches such as the combination of the quantum dot sensitization, chemical doping/loading the metal or the narrow gap semiconductor coupling to enhance light absorption and obtain a higher PEC efficiency [6–8]. These works aim to create acceptor states above the valence band (VB) or donor states below the conduction band (CB) of TiO_2 [9]. Recently, a new strategy to generate a new form of TiO_2 which is called black TiO_2, with self-defect states inside its energy structure playing role as carrier traps below the CB of TiO_2 to narrow the band gap for boosting the interaction of the material with the light irradiation [10]. Besides, these defect states have contributed to the increase of carrier lifetime impressively for excellent photocatalytic activity and PEC efficiency.

In this study, we used the hydrothermal method to reduce the pristine TNAs to the black TNAs. After that, we survey the electrochemical characterizations of the black TNAs and compare with the pristine TNAs.

II. EXPERIMENT

Chemicals and materials

Titanium foils (Ti, 0.25 mm thick, 99.6%), ammonium fluoride (99.9%), ethylene glycol (99.9%), sodium borohydride (99%), potassium hydroxide (99.9%)

Preparation of materials

TNAs were prepared by 2 steps of the anodization of 2 cm^2 Ti sheets. The electrolyte includes ethylene glycol, distilled water (10 vol %), and NH_4F (0.5 wt. %). The first step of anodization process was conducted for 2 h, then sonicating before doing the second step of anodization in 30 min (using an applied potential of 30 V DC for both of 2 steps). After that, the sample was calcinated at 450^oC in 2 h for crystallization. After calcination, the TNAs sheet then treated by hydrothermal method in 1 M $NaBH_4$ solution at 50^oC for 12 h, then cleansing by distilled water to form black TNAs.

Characterizations of materials

The morphology of the material was determined by the scanning electron microscopy (SEM) image. The vibration mode of molecules was detected by Raman spectroscopy using a Raman spectrophotometer, Horiba XploraOne (λ =532 nm) and FT-IR spectroscopy using a FT-IR spectrophotometer, JASCO-4700. The optical characterization was analyzed by diffuse reflectance spectroscopy (DRS) over the wavelength range of 200–800 nm using an UV-Vis spectrometer (JASCO-V550). Photoluminescence (PL) spectra were performed at the room temperature, using a Horiba Jobin-Yvon Nanolog instrument (Xe lamp, $\lambda = 475$ nm) to determine the defects of materials. The electrochemical characterization with cyclic voltammogram (CV) of materials was conducted in an electrochemical workstation (Biologic SP240) with three electrodes including a Pt wire counter electrode, an Ag/AgCl reference electrode in 1 M KOH solution.

III. RESULTS AND DISCUSSION

Characterizations of materials

The morphology of the materials was observed by SEM images and indicated on Fig. 1. Figure 1 shows the morphology of the materials is the tubular structure with the uniform shape both the pristine TNAs (Fig. 1a) and the black TNAs (Fig. 1b). The average diameter of the tubular TiO_2 is about 80-100 nm. After the reduction process, the morphology of the black TNAs almost didn't change compare to the pristine TNAs.

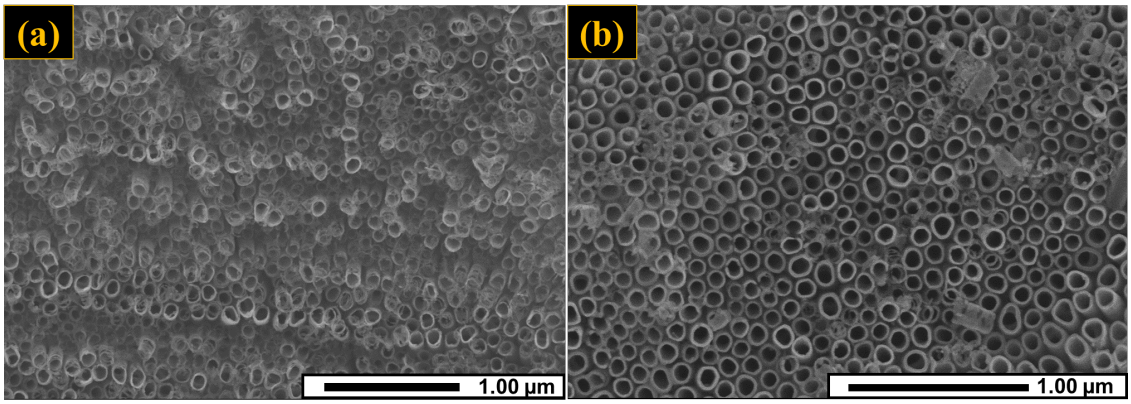

Fig. 1. SEM images of TNAs (a) and black TNAs (b).

In order to determine the formation of TiO_2, FT-IR spectrum has been used and the results were shown in Fig. 2. The appearance of the vibration modes in the region from 500 – 800 cm^{-1} assigning to the vibration of Ti-O, which are the characteristic peaks of TiO_2 for both of TNAs and black TNAs [11]. However, the characteristic peaks of TiO_2 in the FTIR spectrum of black TNAs have shifted to a higher wavenumber, this can be contributed to the formation of Ti^{3+} states in the structure of TNAs to form black TNAs. Besides, the peaks at 3400 cm^{-1}, 1620 cm^{-1} assign to bending vibration of O-H that implies absorbed water on TNAs and black TNAs surface and the peak obtained at 2341 cm^{-1} related to the vibration of CO_2 gas that absorbed on black TNAs surface.

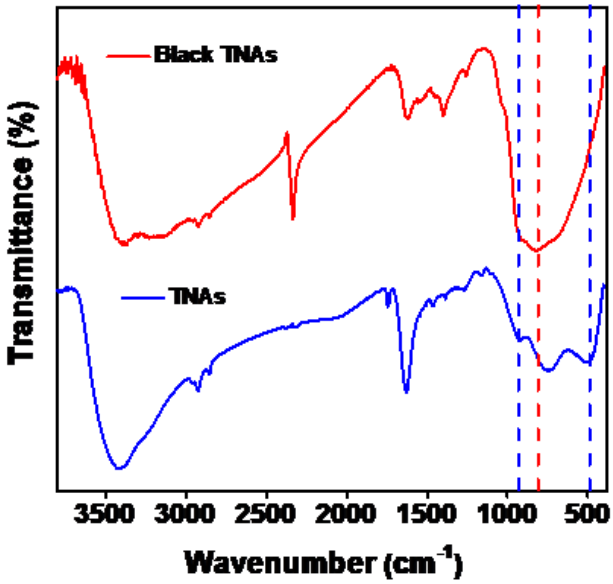

Fig. 2. FT-IR spectra of TNAs and black TNAs.

To investigate the crystalline phase and the effect of the defects on the structure of the black TNAs, Raman spectra have been used and shown in Fig. 3. The obtained peaks of both the pristine TNAs and the black TNAs are almost similar to each other about the Raman shift values. The Raman scattering peaks in the range of 120 cm^{-1} to 700 cm^{-1} could be assigned to the stretching modes of Ti-O bonding in TiO_2 crystal [12]. For the TNAs and the black TNAs, the typical peaks have been obtained at the same wavenumber of 380 cm^{-1}, 505 cm^{-1}, and 631.2 cm^{-1} corresponding to the typical anatase Raman bands of B_{1g}, A_{1g}, and E_g vibration modes, respectively [13]. However, there is a peak of the TNAs at 119 cm^{-1} being shifted strongly to 144 cm^{-1} after the formation of the black TNAs and widening of the FWHM from 18.3 cm^{-1} to 28.4 cm^{-1}. This could be explained due to the disorder in the crystal lattice of the TiO_2 crystal after changing into the black TNAs. The appearance of of Ti^{3+} states in the structure of TiO_2 crystal lattice has led to the shift, which would form a continuum with the conduction band edge and lead to band tail states merging with the valence band, and thus narrowing the band gap.

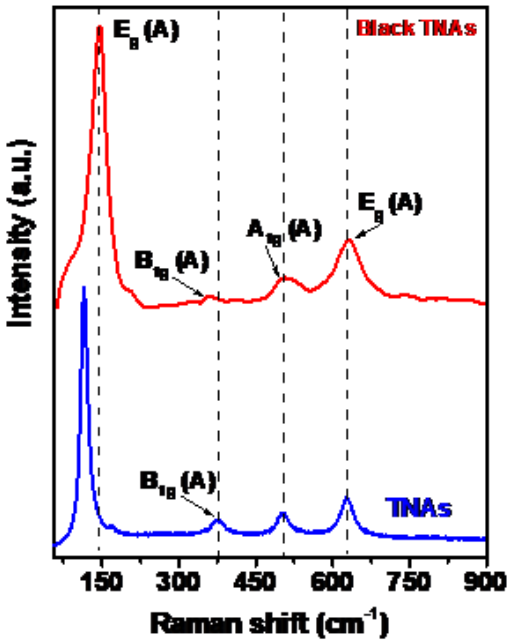

Fig. 3. Raman spectra of TNAs and black TNAs.

Fig. 4 shows the PL spectra of as synthesized samples. As can be seen in Fig. 4a, the PL intensity of black TNAs sample is strongly reduced. This can be explained due to the formation of defect states in the energy structure playing a role as electron traps. The electrons cannot migrate back to the valence band to recombine with the holes leading to reducing the PL intensity and extend the electron lifetime. To give a clearly evidence for the existence of the defect states inside the band structure of black TNAs, the Gaussian fitting curves have been made. The Gaussian fitting curve of the TNAs in Fig. 4b shows two typical peaks at 547 nm (2.27 eV) and 597 nm (2.08 eV) corresponding to the emission of the recombination of the electrons from oxygen vacancy and oxygen vacancy losing one electron states, respectively. The Gaussian fitting curve of the black TNAs in Fig. 4c shows three typical peaks at 522 nm (2.38 eV), 550 nm (2.26 eV) and 595 nm (2.09 eV). Beside the peaks that attributed to the recombination of electrons from oxygen vacancy states, the appearance of the peak at 522 nm of wavelength for the black TNAs has attributed to the luminescence of the recombination of electron from the Ti^{3+} states, which demonstrates for the success of the reduction of Ti^{4+} into Ti^{3+} after the hydrothermal process, and the effect of this kind of defect on the shifting of Raman spectra [14]

Fig. 5 shows the DRS spectra of the pristine TNAs and the black TNAs, the interaction to light of the TNAs sample almost happens in the UV range. However, the black TNAs have a very good interaction to light in both UV range and visible range, with a much higher absorbance compared to TNAs sample.

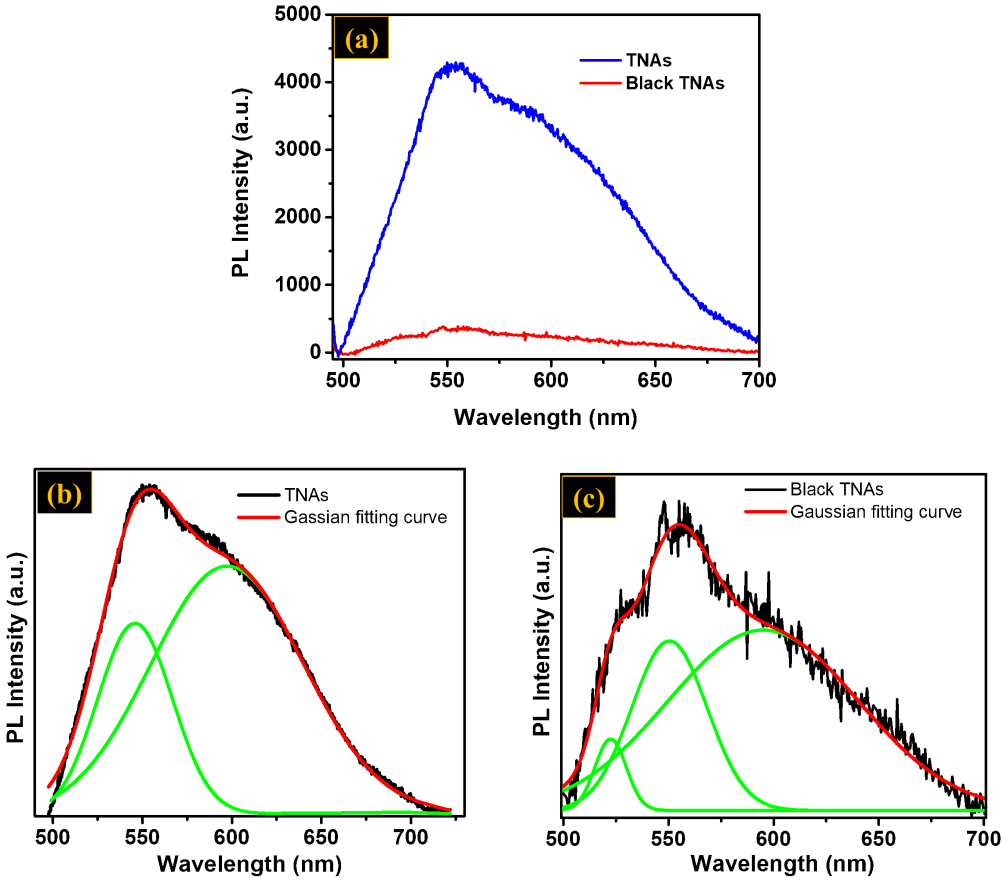

Fig. 4. PL spectra of materials (a) and Gaussian fitting curves of TNAs (b), black TNAs (c).

The band gap energy of the materials can be determined by the following Eq. (1) [15].

$$\alpha h\nu = A(h\nu - E_g)^2 \tag{1}$$

where a, h, ν, A, and E_g are absorption coefficient, Plank's constant, light frequency, a constant, and band gap energy, respectively. The band gap can be obtained by extrapolating to zero a linear fit to a plot of against (often referred to as a Tauc's plot). The estimated optical band gap of the TNAs is about 3.67 eV (Fig. 5b), which is suitable to other publications about TNAs. As shown in Fig. 5c, the estimated optical band gap values of the black TNAs sample is 2.93 eV, clearly indicating for transformation of TNAs into black TNAs with the reduced band gap value. Besides, the color of the TNAs has been changed into black (Fig. 5c).

Fig. 6 demonstrates that the TNAs and the black TNAs have the same behavior in both of two scanning processes. The distance between the absorption peak and the desorption peak of H^+ for the black TNAs is smaller than that of the TNAs, indicating that the black TNAs are less likely to be separated from H^+ leading to increase the hydrogen evolution reaction efficiency.

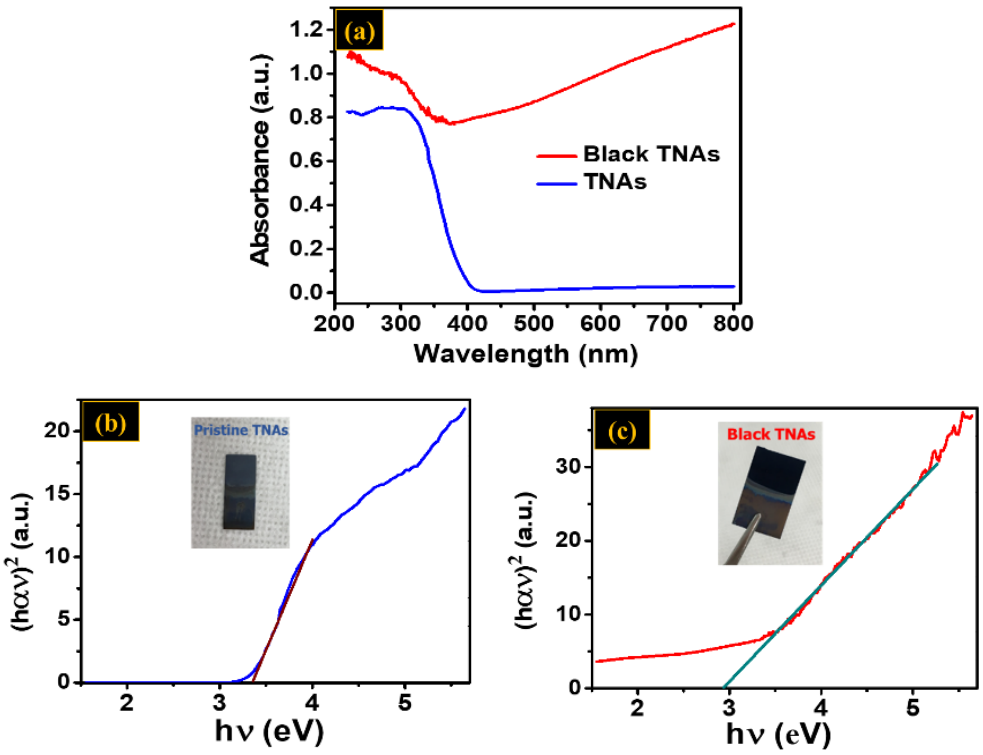

Fig. 5. DRS spectra of materials (a), Kubelka – Munk plots of TNAs (b) and black TNAs (c)

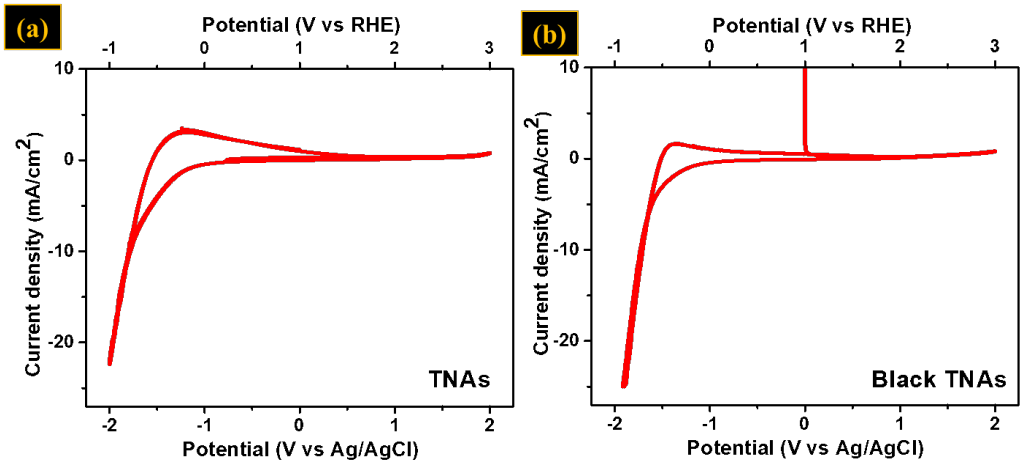

Fig. 6. CV of the TNAs (a) and the black TNAs (b).

In alkaline solutions, the electrolyte cation is probably the charge balancing, therefore, in the first process of scanning, from the positive potential to the negative potential, materials are attributed to filling of surface states below the conduction band, according to Eq. (2) [16, 17]:

$$Ti^{IV}O_2 + e^- + H^+ \longleftrightarrow Ti^{IV}O_2(e^-_{CB})(H^+) \quad (2)$$

Then, the reaction happens to reduce Ti(IV) to Ti(III), according to Eq. (3):

$$Ti^{IV}O_2 + e^- + H^+ \longleftrightarrow Ti^{III}O_2\,(H^+) \quad (3)$$

The TiO(OH) could be formed in alkaline solution and the most critical reaction in this process is the adsorption of H^+ into the materials to form hydrogen gas. Usually, the current at nagative potential increases exponentially, and eventually, hydrogen evolution will be taken by reduction of water. At negative potential value, the reduction reaction of H^+ occurred with the presence of the current formation.

In the reversed period, the TNAs and the black TNAs have a peak in the oxidation range after starting the reversed scan. However, this peak was attributed to H^+ realeased, and adsorbed on the surface of the materials.

IV. CONCLUSIONS

In summary, the black TNAs have been successfully prepared by a simple hydrothermal method with the uniform tubular structure on the Ti substrate. The defects such as Ti^{3+} and oxygen vacancies have been obtained in the black TNAs sample, which enhancing the interaction of the materials to the light irradiation and the electron lifetime. The results show that the as-synthesized samples show a dramatically enhanced light absorption to the visible light region and substantially enhanced electron density in the entire potential window. The black TNAs are less likely to be separated from H^+ leading to increase the hydrogen evolution reaction efficiency.

ACKNOWLEDGMENTS

This research is funded by the University of Science, Vietnam National University Ho Chi Minh City (VNU-HCM) and the CM Thi Laboratory.

REFERENCES

[1] A. Fujishima and K. Honda, *Nature* **238** (1972) 37.
[2] M. Grätzel, *Nature* **414** (2001) 338.
[3] G. Di Carlo, G. Calogero, M. Brucale, D. Caschera, T. de Caro, G. Di Marco and G. M. Ingo, *J. Alloys Compd.* **609** (2014) 116.
[4] L. Aïnouche, L. Hamadou, A. Kadri, N. Benbrahim and D. Bradai, *Sol. Energy Mater. Sol. Cells* **151** (2016) 179.
[5] C. Jiang, S. J. Moniz, A. Wang, T. Zhang and J. Tang, *Chem. Soc. Rev.* **46** (2017) 4645.
[6] J. H. Park, O. O. Park and S. Kim, *App. Phys. Lett.* **89** (2006) 163106.
[7] Q. Gui, Z. Xu, H. Zhang, C. Cheng, X. Zhu, M. Yin, Y. Song, L. Lu, X. Chen and D. Li, *ACS Appl. Mater. Interfaces* **6** (2014) 17053.
[8] Y.-Q. Zhang, D.-K. Ma, Y.-G. Zhang, W. Chen and S.-M. Huang, *Nano Energy* **2** (2013) 545.
[9] G. B. Soares, R. A. P. Ribeiro, S. R. De Lazaro and C. Ribeiro, *RSC Adv.* **6** (2016) 89687.
[10] S. Chen, Y. Xiao, Y. Wang, Z. Hu, H. Zhao and W. Xie, *Nanomater.* **8** (2018) 245.
[11] A. M. Peiró, J. Peral, C. Domingo, X. Domènech and J. A. Ayllón, *Chem. Mater.* **13** (2001) 2567.
[12] M. Mangrola and V. Joshi, *Mater. Today: Proceedings* **4** (2017) 3832.
[13] P. Ramasamy, D.-H. Lim, J. Kim and J. Kim, *RSC Adv.* **4** (2014) 2858.

[14] D. Cristiana, P. Gianfranco, S. Annabella et al., *J. Phys. Chem. C* **113** (2009) 20543.
[15] J. Tauc, *Mater. Res. Bull.* **3** (1968) 37.
[16] T. Berger, T. Lana-Villarreal, D. Monllor-Satoca and R. Gómez, *Electrochem. Commu.* **8** (2006) 1713.
[17] T. Berger, T. Lana-Villarreal, D. Monllor-Satoca and R. Gomez, *J. Phys. Chem. C* **111** (2007) 9936.